LETTERS

AMPK regulates energy expenditure by modulating NAD$^+$ metabolism and SIRT1 activity

Carles Cantó[1,2], Zachary Gerhart-Hines[3], Jerome N. Feige[1], Marie Lagouge[1], Lilia Noriega[1,2], Jill C. Milne[4], Peter J. Elliott[4], Pere Puigserver[3] & Johan Auwerx[1,2,5]

AMP-activated protein kinase (AMPK) is a metabolic fuel gauge conserved along the evolutionary scale in eukaryotes that senses changes in the intracellular AMP/ATP ratio[1]. Recent evidence indicated an important role for AMPK in the therapeutic benefits of metformin[2,3], thiazolidinediones[4] and exercise[5], which form the cornerstones of the clinical management of type 2 diabetes and associated metabolic disorders. In general, activation of AMPK acts to maintain cellular energy stores, switching on catabolic pathways that produce ATP, mostly by enhancing oxidative metabolism and mitochondrial biogenesis, while switching off anabolic pathways that consume ATP[1]. This regulation can take place acutely, through the regulation of fast post-translational events, but also by transcriptionally reprogramming the cell to meet energetic needs. Here we demonstrate that AMPK controls the expression of genes involved in energy metabolism in mouse skeletal muscle by acting in coordination with another metabolic sensor, the NAD$^+$-dependent type III deacetylase SIRT1. AMPK enhances SIRT1 activity by increasing cellular NAD$^+$ levels, resulting in the deacetylation and modulation of the activity of downstream SIRT1 targets that include the peroxisome proliferator-activated receptor-γ coactivator 1α and the forkhead box O1 (FOXO1) and O3 (FOXO3a) transcription factors. The AMPK-induced SIRT1-mediated deacetylation of these targets explains many of the convergent biological effects of AMPK and SIRT1 on energy metabolism.

AMPK is a critical regulator of mitochondrial biogenesis in response to energy deprivation[6]. Although the mechanisms by which AMPK modulates mitochondrial gene expression are not entirely elucidated, they seem to require the peroxisome proliferator-activated receptor-γ coactivator 1α (PGC-1α), either by increasing its expression[7] or direct phosphorylation[8]. Because PGC-1α is also activated by SIRT1-mediated deacetylation[9–12], we speculated that AMPK alters PGC-1α activity by changing its acetylation status. Treatment of C2C12 myotubes with the AMPK activator 5-aminoimidazole-4-carboxamide-1-β-D-riboside (AICAR) decreased PGC-1α acetylation after 4 h of treatment (Fig. 1a). Unrelated AMPK activators (Supplementary Fig. 1a, b), such as resveratrol[13,14], metformin[3], dinitrophenol (DNP)[15] and A-769662[16], also decreased PGC-1α acetylation (Fig. 1b and Supplementary Fig. 1c). Furthermore, overexpression of a constitutively active form of AMPKα$_1$ led to a robust deacetylation of PGC-1α that could not be further enhanced by AICAR (Fig. 1c). In contrast, when a dominant negative form of AMPKα$_i$ was overexpressed, AICAR was unable to deacetylate PGC-1α (Fig. 1c). The activation of AMPK hence triggers PGC-1α deacetylation in C2C12 myotubes.

To validate these observations *in vivo*, we examined PGC-1α acetylation in hindlimb muscles after a single AICAR injection. PGC-1α acetylation was markedly reduced by AICAR in extensor digitorum longus (EDL) and gastrocnemius, but not in soleus (Fig. 1d). The soleus is an oxidative muscle, where basal PGC-1α activity is presumably higher than in glycolytic muscles such as the EDL. Supporting this hypothesis, basal PGC-1α acetylation levels were lower in soleus than EDL (Supplementary Fig. 2a), explaining why the soleus is refractory to AICAR. AICAR-induced PGC-1α deacetylation in muscle correlated with an increase of PGC-1α target genes (Supplementary Fig. 2b). Consistent with PGC-1α acetylation levels, AICAR had, however, minor effects on mitochondrial gene expression in the soleus (Supplementary Fig. 2c).

We then tested whether AMPK activation through exercise decreases PGC-1α acetylation. An exhaustive single bout of treadmill running transiently activated AMPK (Supplementary Fig. 3a) and induced PGC-1α deacetylation with a maximal effect 3 h after ending exercise (Fig. 1e). As observed with AICAR infusion, the soleus was refractory to exercise-induced PGC-1α deacetylation (Fig. 1e) despite being effectively recruited, as indicated by the diminished glycogen levels and increased AMPK activity (Supplementary Fig. 3b, c). The decrease in PGC-1α acetylation in EDL and gastrocnemius, but not in soleus, translated to a marked induction of PGC-1α target genes, such as carnitine palmitoyltransferase 1b (*Cpt1b*), pyruvate dehydrogenase kinase 4 (*Pdk4*) or *Glut4* (also called *Slc2a4*; Supplementary Fig. 3d), whereas these genes only minimally responded in soleus (Supplementary Fig. 3e). Together, these results physiologically correlate AMPK activation, PGC-1α deacetylation and PGC-1α activity.

Because SIRT1 interacts with and deacetylates PGC-1α[9,11], we next evaluated whether SIRT1 mediates the AICAR-induced deacetylation of PGC-1α. Pre-treatment of C2C12 myotubes with nicotinamide (NAM), a type III histone deacetylase inhibitor[17], blocked AICAR-induced PGC-1α deacetylation (Supplementary Fig. 4). Furthermore, AICAR failed to decrease PGC-1α acetylation when SIRT1 expression was knocked down with a short hairpin RNA[9] (shRNA; Fig. 2a) or genetically ablated, as in *Sirt1*$^{-/-}$ mouse embryonic fibroblasts (MEFs)[18] (Fig. 2b). The lack of SIRT1 did not affect AICAR-induced AMPK phosphorylation in any of these models (Fig. 2c, d). The protein levels of SIRT2 and SIRT3, the closest homologues of SIRT1, were not affected by reduced SIRT1 expression (Supplementary Fig. 5), ruling out their implication in the blunted response to AICAR.

We next explored whether PGC-1α deacetylation influences AMPK-induced PGC-1α transcriptional activity. Because PGC-1α positively autoregulates its own promoter[19], we monitored PGC-1α activity by transiently transfecting a luciferase reporter under the control of the *Pgc1-α* (also called *Ppargc1a*) promoter, in the absence/presence of PGC-1α and a *Sirt1* shRNA. AICAR robustly increased PGC-1α action on its own promoter in both C2C12 myocytes (Fig. 3a) and *Sirt1*$^{+/+}$ mouse embryonic fibroblasts (Fig. 3b). This increase was

[1]Institut de Génétique et de Biologie Moléculaire et Cellulaire, CNRS/INSERM/ULP, 67404 Illkirch, France. [2]Ecole Polytechnique Fédérale de Lausanne, CH1015 Lausanne, Switzerland. [3]Dana-Farber Cancer Institute and Department of Cell Biology, Harvard Medical School, Boston, Massachusetts 02115, USA. [4]Sirtris Pharmaceuticals Inc., Cambridge, Massachusetts 02139, USA. [5]Institut Clinique de la Souris, BP10142, 67404 Illkirch, France.

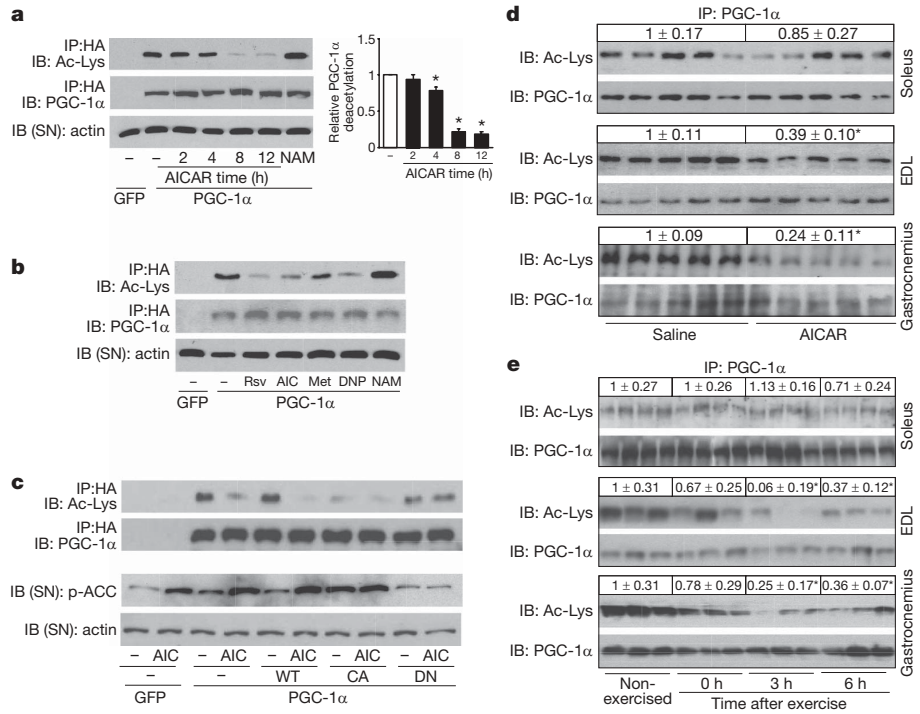

Figure 1 | Activation of AMPK triggers PGC-1α deacetylation in C2C12 myotubes and skeletal muscle. **a**, **b**, C2C12 myotubes infected with adenoviruses for GFP or Flag–HA-tagged PGC-1α (PGC-1α) were treated with vehicle (−), AICAR (0.5 mM, 2–8 h) or nicotinamide (NAM; 5 mM; 12 h). Then, acetyl-lysine levels were checked on PGC-1α immunoprecipitates (IP). The supernatant (SN) was blotted against actin as input control. Relative quantification of PGC-1α acetylation is shown on the right. **b**, As in **a**, but myotubes were treated for 8 h with vehicle (−), resveratrol (Rsv; 50 μM), AICAR (AIC), metformin (Met; 1 mM), DNP (0.5 mM) or NAM. **c**, C2C12 myotubes were infected with adenoviruses encoding GFP, PGC-1α and wild-type (WT), constitutively active (CA) or dominant negative (DN) forms of AMPKα$_1$. After AICAR treatment, total lysates were analysed as in **a**. **d**, PGC-1α acetylation was measured on total protein (soleus and EDL) or nuclear extracts (gastrocnemius) from muscles of mice treated with AICAR or saline. Relative acetylation levels are shown on top of the panels. **e**, Soleus, EDL and gastrocnemius were obtained from non-exercised or exercised mice at 0, 3 or 6 h after cessation of exercise, and analysed as in **d**. Values are expressed as mean ± s.e.m. Asterisks indicate statistical difference versus corresponding vehicle, saline or non-exercised group at $P < 0.05$.

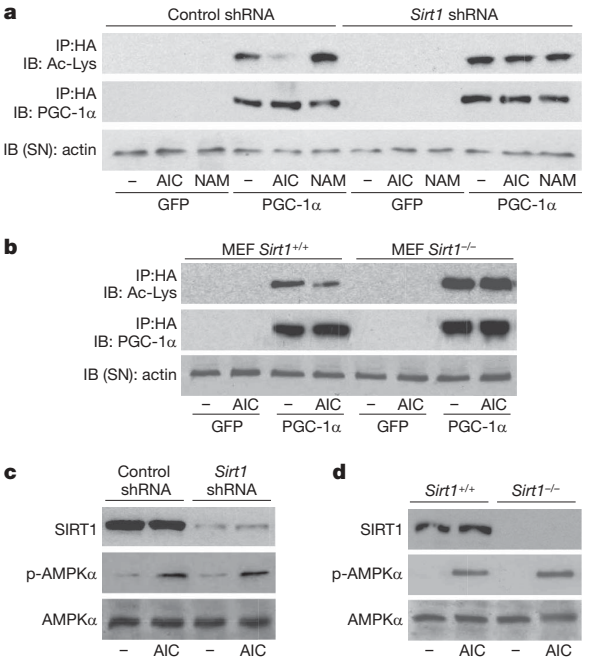

Figure 2 | SIRT1 mediates AMPK-induced PGC-1α deacetylation. **a**, **c**, C2C12 myocytes were infected with adenoviruses encoding GFP, PGC-1α and either control or *Sirt1* shRNAs. After 8 h (**a**) or 1 h (**c**) of AICAR treatment, PGC-1α acetylation and AMPK phosphorylation were analysed. **b**, **d**, *Sirt1*$^{+/+}$ and *Sirt1*$^{-/-}$ MEFs were infected with GFP and Flag–HA–PGC-1α and treated for 8 h (**b**) or 1 h (**d**) with AICAR to test PGC-1α acetylation and AMPK phosphorylation.

reduced over 60% when SIRT1 was knocked down in these cells (Fig. 3a, b). Conversely, AICAR only mildly activated PGC-1α in *Sirt1*$^{-/-}$ MEFs, but full AICAR action was recovered when SIRT1 was reintroduced (Fig. 3c). The lack of SIRT1 also compromised AICAR-induced PGC-1α-dependent transcriptional activity on promoters of other target genes, such as *Pdk4*[20] and *Mcad*[21] (also called *Acadm*; Supplementary Fig. 6a, b). The overexpression of the constitutively active PGC-1α R13 mutant, where the 13 acetylation sites are mutated, activated the *Pgc-1α* promoter, which could not be further enhanced by AICAR or inhibited by a *Sirt1* shRNA (Supplementary Fig. 6c). This indicates that SIRT1 and the deacetylation of PGC-1α are necessary for AMPK to increase PGC-1α activity.

We then tested whether the lack of SIRT1 affects AICAR-induced expression of genes related to mitochondrial metabolism and fatty acid utilization, which are under the control of PGC-1α. AICAR-induced expression of genes involved in mitochondrial gene expression (such as oestrogen-related receptor-α (*Esrra*) and *Pgc-1α*), mitochondrial architecture and electron transport (such as cytochrome *c* (*Cyc*), cytochrome *c* oxidase IV (*Cox4*) and mitofusin-2 (*Mfn2*)), and in fatty acid utilization (such as *Cpt1b* and *Pdk4*), was either prevented or robustly attenuated by knocking down SIRT1 expression in C2C12 myotubes (Fig. 3d and Supplementary Fig. 7) or deletion of the *Sirt1* gene in MEFs (Supplementary Fig. 8). The lack of SIRT1 also impaired the action of metformin on the expression of this gene set (Supplementary Fig. 9). In contrast, AICAR was unable to increase further the expression of PGC-1α targets in C2C12 myotubes overexpressing the PGC-1α R13 mutant (Supplementary Fig. 10). Together, these data indicate that, to a large extent, AMPK regulates the expression of mitochondrial and lipid metabolism genes through the modulation of PGC-1α activity by SIRT1.

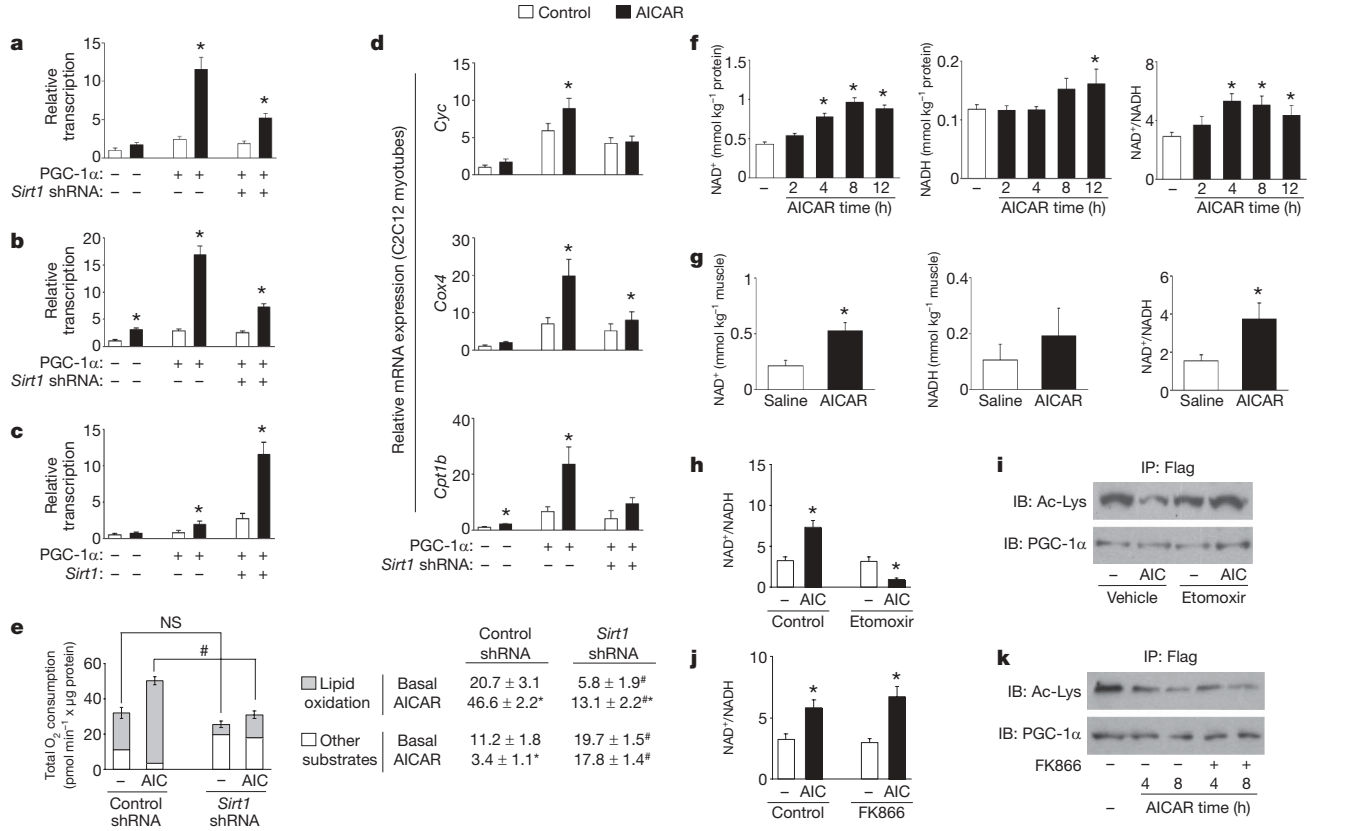

Figure 3 | AICAR modulates PGC-1α-dependent transcriptional activity, mitochondrial gene expression and oxygen consumption through SIRT1 and NAD^+ metabolism. **a**, C2C12 myocytes were transfected with a 2-kb mouse PGC-1α (mPGC-1α) promoter luciferase reporter, a plasmid for mPGC-1α and simultaneously infected with adenovirus encoding control or *Sirt1* shRNA. Thirty-six hours later, cells were treated with AICAR (12 h) and reporter activity was determined. **b**, $Sirt1^{+/+}$ MEFs were analysed as in **a**. **c**, $Sirt1^{-/-}$ MEFs were transfected with the 2-kb mPGC-1α reporter and expression plasmids for PGC-1α, SIRT1 or the corresponding empty vectors. Then, cells were treated and analysed as in **a**. **d**, C2C12 myotubes were infected with adenoviruses for GFP, PGC-1α and either control or *Sirt1* shRNAs. After AICAR treatment, target mRNAs were analysed by qRT–PCR. **e**, O_2 consumption in C2C12 myotubes infected with PGC-1α, and either control or *Sirt1* shRNAs. Total length of the bar equals total O_2 consumption. The white part of the bar is the O_2 consumption in each group when treated with etomoxir (1 mM). Therefore, the grey part represents lipid oxidation-derived O_2 consumption. Values for O_2 consumption due to the oxidation of lipids and other substrates are indicated on the right. **f**, NAD^+ and NADH content in C2C12 myotubes treated with AICAR for the times indicated. **g**, Whole tibialis anterior muscles from mice treated with saline or AICAR were used for the measurement of NAD^+ and NADH. **h**, **i**, C2C12 myotubes pre-incubated with vehicle or etomoxir (50 μM) for 1 h were treated with either vehicle (−) or AICAR (AIC). Then, NAD^+ and NADH (**h**) or PGC-1α acetylation levels (**i**) were measured. **j**, **k**, As in **h**, **i**, but using FK866 (10 nM) instead of etomoxir. All values are expressed as mean ± s.e.m. Asterisks indicate statistical difference versus vehicle/saline group at $P < 0.05$. Hash symbols indicate statistical difference versus respective control shRNA group at $P < 0.05$.

SIRT1 also had a major role in the ability of AMPK to increase mitochondrial respiration, as the long-term effects of AICAR on cellular O_2 consumption, a readout of oxidative metabolism, were severely blunted by knocking down SIRT1 (Fig. 3e). Thus, we determined the contribution of lipid oxidation to total O_2 consumption by blocking mitochondrial fatty acid uptake with etomoxir. Confirming previous observations[10], knocking down SIRT1 severely decreased lipid oxidation and increased the oxidation of alternative substrates (Fig. 3e). In control cells, AICAR markedly increased lipid oxidation-driven O_2 consumption, whereas it almost completely blocked the oxidation of other substrates, such as glucose. When SIRT1 expression was knocked down, AICAR action on lipid oxidation was blunted and, additionally, AICAR was unable to decrease O_2 consumption derived from the other substrates (Fig. 3e). In line with this, direct measurement of oleate oxidation confirmed that the chronic effects of AICAR on lipid oxidation were blunted in myotubes where SIRT1 expression was knocked down (Supplementary Fig. 11). The lack of SIRT1 hence alters the long-term actions of AICAR on lipid oxidation and global cellular O_2 consumption.

As AICAR or metformin cannot directly activate SIRT1 (Supplementary Fig. 12), our data suggest that AMPK signalling modulates SIRT1 activity indirectly. No changes in SIRT1 protein levels were detected after 8 h of AICAR (Supplementary Fig. 13a), when PGC-1α is already maximally deacetylated, indicating that changes in activity where not due to increased SIRT1 abundance. We could not observe interaction of AMPK with SIRT1 up to 8 h after AICAR, either in the presence or absence of PGC-1α (Supplementary Fig. 13b). Finally, AMPK could not phosphorylate SIRT1 *in vitro* either on the full-length protein (Supplementary Fig. 13c) or on different GST fragments (Supplementary Fig. 13d). These results suggest that AMPK regulates SIRT1 action by indirect mechanisms.

Because SIRT1 deacetylase activity is driven by NAD^+ levels[22], we examined whether AMPK indirectly activates SIRT1 by altering the intracellular NAD^+/NADH ratio. Supporting this hypothesis, AICAR increased the NAD^+/NADH ratio in C2C12 myotubes and in skeletal muscle (Fig. 3f, g, respectively). The increase in NAD^+/NADH ratio was evident 4 h after AICAR in C2C12 myotubes, and remained elevated after 12 h (Fig. 3f), a timing that perfectly correlates with PGC-1α deacetylation (Fig. 1a). Activation of AMPK by metformin, DNP, or overexpression of a constitutively active form of $AMPK\alpha_1$ also increased the NAD^+/NADH ratio (Supplementary Fig. 14a, b). A significant increase in NAD^+ was also evident 3 h after exercise in tibialis anterior muscle, further supporting the hypothesis that changes in NAD^+ levels translate AMPK effects onto SIRT1 activity (Supplementary Fig. 14c).

To determine how AMPK acutely increases the NAD^+/NADH ratio, we pharmacologically targeted different possible sources of cellular NAD^+ production. Inhibition of the glycolytic enzyme lactate dehydrogenase with oxamic acid did not affect the ability of AICAR to increase NAD^+ levels and the NAD^+/NADH ratio (Supplementary Fig. 15a). In contrast, inhibition of mitochondrial fatty acid oxidation with etomoxir was enough to hamper the increase in NAD^+/NADH induced by AMPK (Fig. 3h and Supplementary Fig. 15b), indicating that an increase in mitochondrial β-oxidation is required for AMPK to increase the NAD^+/NADH ratio. Supporting the role of NAD^+/NADH ratio on SIRT1 activity, etomoxir also abolished AMPK-induced PGC-1α deacetylation (Fig. 3i),

SIRT1 activity is inhibited by NAM, a product of the deacetylation reaction catalysed by the sirtuins[17]. NAM can be cleared and enzymatically reconverted into NAD^+ through the NAD^+ salvage pathway, the initial rate-limiting step of which is catalysed in mammals by nicotinamide phosphoribosyltransferase (NAMPT)[23]. Acute blockage of NAMPT activity with the specific inhibitor FK866[24], however, did not affect AICAR's capacity to modulate PGC-1α acetylation or NAD^+/NADH ratio up to 8 h after treatment (Fig. 3j, k and Supplementary Fig. 15c). These results apparently conflict with observations indicating that NAMPT can link AMPK and SIRT1 activities[25]. These differences may be explained by the fact that a chronic knock down of NAMPT may constitutively inhibit SIRT1 due to reduced intracellular NAM clearance[17]. Supporting this speculation, knock down of NAMPT for 48 h promotes PGC-1α hyperacetylation (Supplementary Fig. 16). The use of FK866 dissociates the direct effects of acute NAMPT inhibition from those of indirect SIRT1 inhibition and indicates that AMPK initially regulates the NAD^+/NADH ratio and SIRT1 activity independently of NAMPT. These results, however, do not rule out that NAMPT could participate to sustain the actions of AMPK on SIRT1.

Whereas it has been reported that AMPK activates PGC-1α through direct phosphorylation[8], our data show that deacetylation of PGC-1α on AMPK activation is also required to activate PGC-1α. To understand how both post-translational modifications intertwine, we used the PGC-1α 2A mutant lacking the two AMPK phosphorylation sites[8]. Mutation of these sites markedly reduced deacetylation of PGC-1α by AICAR (Fig. 4a), and, consistently, blunted AICAR action on the expression of mitochondrial genes (Fig. 4b). The expression of the PGC-1α 2A mutant, however, did not alter AICAR action on the NAD^+/NADH ratio, which increased to a similar extent as in myocytes expressing wild-type PGC-1α (Fig. 4c and Supplementary Fig. 17). This suggested that the activation of SIRT1 by AMPK should theoretically be unaffected by the PGC-1α 2A mutant and, consequently, still have an impact on other SIRT1 substrates beyond PGC-1α, like the FOXO transcription factors[26]. AICAR treatment triggered the deacetylation of endogenous FOXO1 (Fig. 4d), as well as other members of the FOXO family, such as FOXO3a (Supplementary Fig. 18), in C2C12 myotubes. The deacetylation of FOXO1 in response to AICAR was similar in myocytes expressing wild-type PGC-1α or the 2A mutant (Fig. 4e), demonstrating that the PGC-1α 2A mutation only alters PGC-1α deacetylation but not general SIRT1 activation in response to AICAR. Hence, the data suggest a scenario where phosphorylation of PGC-1α constitutes a priming signal for subsequent deacetylation by SIRT1 (Fig. 4f). Notably, AMPK can also phosphorylate the FOXO transcription factors[27], which are also targets for SIRT1 deacetylation[26]. It is therefore tempting to speculate that the coordinated sequential actions of AMPK and SIRT1 could be a conserved mechanism for AMPK to modulate the specificity among SIRT1 targets, with phosphorylation discriminating which substrates should be deacetylated and preventing random deacetylation.

This work demonstrates that deacetylation of PGC-1α is a key mechanism by which AMPK triggers PGC-1α activity in cultured myotubes and in skeletal muscle. We also unveil SIRT1 as a key, albeit not the sole, mediator of AMPK action on PGC-1α transcriptional activity, the expression of mitochondrial and lipid metabolism genes, and O_2 consumption (Fig. 3). The acute actions of AMPK on lipid oxidation alter the balance between cellular NAD^+ and NADH,

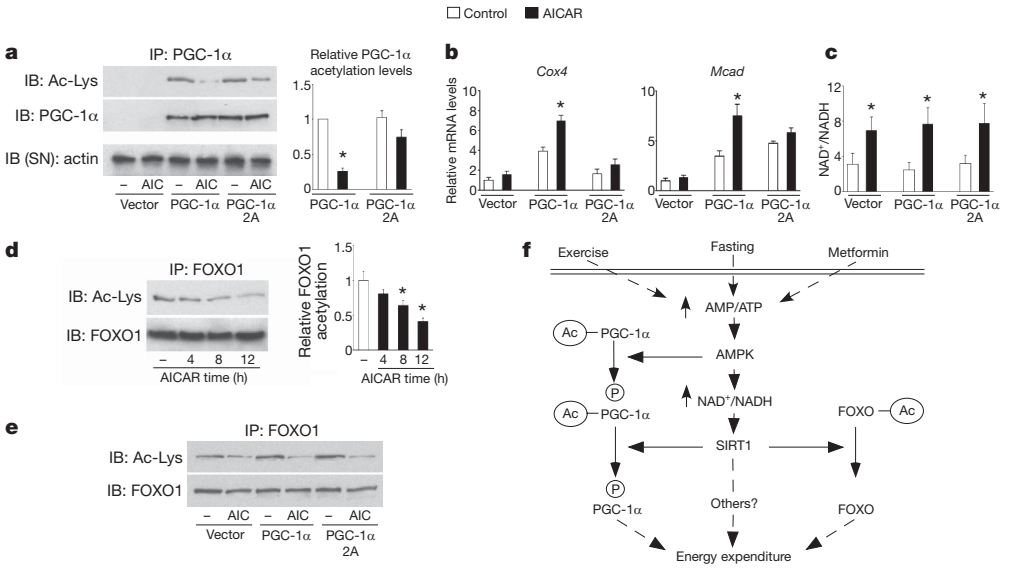

Figure 4 | The PGC-1α phosphorylation mutant is resistant to deacetylation. **a**, C2C12 myocytes were transfected with the wild-type or the 2A mutant form of PGC-1α, using empty vector as control. After 36 h, cells were treated with AICAR and total lysates were used to test PGC-1α acetylation. Relative acetylation levels of PGC-1α are shown on the right. **b**, Cells were treated as in **a**, and, after AICAR treatment, target mRNA levels were analysed by RT–qPCR. **c**, Cells were treated as in **a**, and acidic or alkali lysates were obtained to measure NAD^+ and NADH. **d**, C2C12 myotubes were treated with AICAR for the times indicated. Then, total protein lysates were used for immunoprecipitation of FOXO1. Relative FOXO1 acetylation is shown on the right. **e**, As in **a**, but immunoprecipitations were performed against FOXO1. **f**, Scheme illustrating the convergent actions of AMPK and SIRT1 on PGC-1α. Pharmacological (metformin) and physiological (fasting or exercise) activation of AMPK in muscle triggers an increase in the NAD^+/NADH ratio, which activates SIRT1. AMPK also induces the phosphorylation of PGC-1α and primes it for subsequent deacetylation by SIRT1. The impact of AMPK and SIRT1 on the acetylation status of PGC-1α and other transcriptional regulators, such as the FOXO family of transcription factors, will then modulate mitochondrial function and lipid metabolism. All values are presented as mean ± standard error. Asterisks indicate statistical difference versus corresponding vehicle group at $P < 0.05$.

which acts as a messenger to activate SIRT1. This study constitutes a step forward in the understanding of the mechanisms by which AMPK transcriptionally regulates energy expenditure. The implication of SIRT1 in the transcriptional actions of AMPK provides a possible explanation for the overlapping metabolic effects of SIRT1 and AMPK activators[7,12,16,28,29]. Furthermore, the interplay between SIRT1 and AMPK might be reciprocal, as specific SIRT1 agonists promote fatty acid oxidation and indirectly activate AMPK through metabolic adaptations[29]. Hence, the interdependent regulation of SIRT1 and AMPK provides a finely tuned amplification mechanism for energy homeostasis under low nutrient availability. Together, these findings constitute a conciliatory view of the possible implications of AMPK and SIRT1 on the pleiotropic beneficial effects of calorie restriction on metabolic homeostasis and lifespan, where both enzymes were known to participate, but never linked.

METHODS SUMMARY

Reagents and materials. The origin of all chemicals, antibodies, plasmids and adenoviruses is listed in Methods.

Cell culture. C2C12 skeletal muscle cells were grown and differentiated as described[12]. C2C12 cells were considered as myotubes after 96 h of differentiation. Differentiation medium was supplemented with 0.1 mM oleic acid. Unless otherwise stated, AICAR treatments lasted 8 h. Additional cell culture procedures can be found in Methods.

Animal experiments. All animals were purchased from Charles River. Eight-week-old C57BL/6J male mice were injected subcutaneously with AICAR ($1.0\,mg\,g^{-1}$ body weight) or saline. AICAR was dissolved in $50\,mg\,ml^{-1}$ saline. Injection time was at the start of the dark cycle, and animals had free access to food and water. AICAR injection did not alter food intake during the 12 h period (data not shown). Twelve hours after injection, hindlimb muscles were collected and immediately frozen in liquid nitrogen. The exercise protocol used can be found in Methods.

Statistics. Statistical analyses were performed with the Student's *t*-test for independent samples (nonparametric), and data are expressed as mean ± standard error unless otherwise specified. P value <0.05 was considered as statistically significant. In cell-based experiments the n ranged from 4 to 12 independent experiments. In animal-based studies, $n = 8$–10 animals per group.

Additional experimental procedures can be found in Methods.

Full Methods and any associated references are available in the online version of the paper at www.nature.com/nature.

Received 22 October 2008; accepted 22 January 2009.
Published online 4 March 2009.

1. Hardie, D. G. AMP-activated/SNF1 protein kinases: conserved guardians of cellular energy. *Nature Rev. Mol. Cell Biol.* **8,** 774–785 (2007).
2. Shaw, R. J. *et al.* The kinase LKB1 mediates glucose homeostasis in liver and therapeutic effects of metformin. *Science* **310,** 1642–1646 (2005).
3. Zhou, G. *et al.* Role of AMP-activated protein kinase in mechanism of metformin action. *J. Clin. Invest.* **108,** 1167–1174 (2001).
4. Fryer, L. G., Parbu-Patel, A. & Carling, D. The Anti-diabetic drugs rosiglitazone and metformin stimulate AMP-activated protein kinase through distinct signaling pathways. *J. Biol. Chem.* **277,** 25226–25232 (2002).
5. Barnes, B. R. *et al.* Changes in exercise-induced gene expression in 5′-AMP-activated protein kinase γ3-null and γ3 R225Q transgenic mice. *Diabetes* **54,** 3484–3489 (2005).
6. Zong, H. *et al.* AMP kinase is required for mitochondrial biogenesis in skeletal muscle in response to chronic energy deprivation. *Proc. Natl Acad. Sci. USA* **99,** 15983–15987 (2002).
7. Suwa, M., Nakano, H. & Kumagai, S. Effects of chronic AICAR treatment on fiber composition, enzyme activity, UCP3, and PGC-1 in rat muscles. *J. Appl. Physiol.* **95,** 960–968 (2003).
8. Jager, S., Handschin, C., St-Pierre, J. & Spiegelman, B. M. AMP-activated protein kinase (AMPK) action in skeletal muscle via direct phosphorylation of PGC-1α. *Proc. Natl Acad. Sci. USA* **104,** 12017–12022 (2007).
9. Rodgers, J. T. *et al.* Nutrient control of glucose homeostasis through a complex of PGC-1α and SIRT1. *Nature* **434,** 113–118 (2005).
10. Gerhart-Hines, Z. *et al.* Metabolic control of muscle mitochondrial function and fatty acid oxidation through SIRT1/PGC-1α. *EMBO J.* **26,** 1913–1923 (2007).
11. Nemoto, S., Fergusson, M. M. & Finkel, T. SIRT1 functionally interacts with the metabolic regulator and transcriptional coactivator PGC-1α. *J. Biol. Chem.* **280,** 16456–16460 (2005).
12. Lagouge, M. *et al.* Resveratrol improves mitochondrial function and protects against metabolic disease by activating SIRT1 and PGC-1α. *Cell* **127,** 1109–1122 (2006).
13. Dasgupta, B. & Milbrandt, J. Resveratrol stimulates AMP kinase activity in neurons. *Proc. Natl Acad. Sci. USA* **104,** 7217–7222 (2007).
14. Baur, J. A. *et al.* Resveratrol improves health and survival of mice on a high-calorie diet. *Nature* **444,** 337–342 (2006).
15. Hayashi, T. *et al.* Metabolic stress and altered glucose transport: activation of AMP-activated protein kinase as a unifying coupling mechanism. *Diabetes* **49,** 527–531 (2000).
16. Cool, B. *et al.* Identification and characterization of a small molecule AMPK activator that treats key components of type 2 diabetes and the metabolic syndrome. *Cell Metab.* **3,** 403–416 (2006).
17. Bitterman, K. J., Anderson, R. M., Cohen, H. Y., Latorre-Esteves, M. & Sinclair, D. A. Inhibition of silencing and accelerated aging by nicotinamide, a putative negative regulator of yeast sir2 and human SIRT1. *J. Biol. Chem.* **277,** 45099–45107 (2002).
18. Chua, K. F. *et al.* Mammalian SIRT1 limits replicative life span in response to chronic genotoxic stress. *Cell Metab.* **2,** 67–76 (2005).
19. Handschin, C., Rhee, J., Lin, J., Tarr, P. T. & Spiegelman, B. M. An autoregulatory loop controls peroxisome proliferator-activated receptor γ coactivator 1α expression in muscle. *Proc. Natl Acad. Sci. USA* **100,** 7111–7116 (2003).
20. Wende, A. R., Huss, J. M., Schaeffer, P. J., Giguere, V. & Kelly, D. P. PGC-1α coactivates PDK4 gene expression via the orphan nuclear receptor ERRα: a mechanism for transcriptional control of muscle glucose metabolism. *Mol. Cell. Biol.* **25,** 10684–10694 (2005).
21. Huss, J. M., Kopp, R. P. & Kelly, D. P. Peroxisome proliferator-activated receptor coactivator-1α (PGC-1α) coactivates the cardiac-enriched nuclear receptors estrogen-related receptor-α and -γ. Identification of novel leucine-rich interaction motif within PGC-1α. *J. Biol. Chem.* **277,** 40265–40274 (2002).
22. Imai, S., Armstrong, C. M., Kaeberlein, M. & Guarente, L. Transcriptional silencing and longevity protein Sir2 is an NAD-dependent histone deacetylase. *Nature* **403,** 795–800 (2000).
23. Revollo, J. R., Grimm, A. A. & Imai, S. The NAD biosynthesis pathway mediated by nicotinamide phosphoribosyltransferase regulates Sir2 activity in mammalian cells. *J. Biol. Chem.* **279,** 50754–50763 (2004).
24. Hasmann, M. & Schemainda, I. FK866, a highly specific noncompetitive inhibitor of nicotinamide phosphoribosyltransferase, represents a novel mechanism for induction of tumor cell apoptosis. *Cancer Res.* **63,** 7436–7442 (2003).
25. Fulco, M. *et al.* Glucose restriction inhibits skeletal myoblast differentiation by activating SIRT1 through AMPK-mediated regulation of Nampt. *Dev. Cell* **14,** 661–673 (2008).
26. Brunet, A. *et al.* Stress-dependent regulation of FOXO transcription factors by the SIRT1 deacetylase. *Science* **303,** 2011–2015 (2004).
27. Greer, E. L. *et al.* The energy sensor AMP-activated protein kinase directly regulates the mammalian FOXO3 transcription factor. *J. Biol. Chem.* **282,** 30107–30119 (2007).
28. Milne, J. C. *et al.* Small molecule activators of SIRT1 as therapeutics for the treatment of type 2 diabetes. *Nature* **450,** 712–716 (2007).
29. Feige, J. N. *et al.* Specific SIRT1 activation mimics low energy levels and protects against diet-induced metabolic disorders by enhancing fat oxidation. *Cell Metab.* **8,** 347–358 (2008).

Supplementary Information is linked to the online version of the paper at www.nature.com/nature.

Acknowledgements This work was supported by grants of CNRS, Ecole Polytechnique Fédérale de Lausanne, INSERM, ULP, NIH (DK59820 and DK069966), EU FP6 (EUGENE2; LSHM-CT-2004-512013) and EU Ideas programme (sirtuins; ERC-2008-AdG-23118). C.C. has been supported by grants of Fondation de la Recherche Medicale (FRM) and EMBO. J.N.F. was supported by a FEBS grant. The authors thank F. Foufelle and P. Ferre, B. Spiegelman, D. P. Kelly, S.-i. Imai, G. Hardie, C. Ammann (Topotarget) and F. Alt for providing materials, and members of the Auwerx and Puigserver laboratories for discussion.

Author Contributions C.C. designed and executed experiments, interpreted data and wrote the manuscript. Z.G.-H., J.C.M., J.N.F., M.L. and L.N. performed experiments and J.N.F. helped with writing. P.J.E. and P.P. provided crucial reagents and helped with data interpretation. J.A. supervised the design and interpretation of the experiments and participated in the writing of the manuscript.

Author Information Reprints and permissions information is available at www.nature.com/reprints. The authors declare competing financial interests: details accompany the full-text HTML version of the paper at www.nature.com/nature. Correspondence and requests for materials should be addressed to J.A. (admin.auwerx@epfl.ch).

METHODS

Exercise protocol. 8-week-old non-fasted C57BL6/J male mice were subjected to a resistance running test, using a variable speed belt treadmill enclosed in a plexiglass chamber with a stimulus device consisting of a shock grid attached to the rear of the belt (Panlab). Animals were acclimatized to the chamber the day preceding the running test. For the habituation, mice run at 21 cm s^{-1} for 10 min with a 5° incline. For the actual test, we used a protocol at 5° incline where, beginning at 18 cm s^{-1}, speed increased gradually by 3 cm s^{-1} every 5 min. The distance run and the number of shocks were monitored during the test, and exhaustion was assumed when mice received more than 50 shocks in a 2.5 min interval. Mice were removed from the treadmill on exhaustion.

Preceding the running test, we randomly subdivided mice into three different groups (8 mice per group): one group that would be killed immediately after the exercise test, another which would be killed 3 h after the exercise test, and, finally, a group that would be killed 6 h after the cessation of exercise. The time and distance run before exhaustion was similar in the three groups (data not shown), around 600 m after 40 min of exercise. Mice killed 3 and 6 h after exercise had free access to food and water once the running protocol was finished.

Reagents and materials. AICAR was purchased from Toronto Research Chemicals. Anti-PGC-1α (H300) and anti-actin goat antibodies were purchased from Santa Cruz Biotechnology Inc. Anti-PGC-1α, anti-acetyl-lysine, anti-AMPKα, anti-phospho-AMPKα (Thr 172) and anti-FOXO1 polyclonal antibodies were purchased from Cell Signaling. Anti-Sir2 and anti-phospho AcetylCoA carboxylase (ACC) (Ser 79) were purchased from Upstate Biotechnology Inc. Anti-NAMPT antibody was purchased from Bethyl laboratories. Anti-Flag (M2) and anti-HA monoclonal antibodies as well as most commonly used chemicals were purchased from Sigma Aldrich. *Nampt* siRNAs were purchased from Dharmacon Inc. The A-769662 compound was a gift from G. Hardie. C. Ammann provided the FK866 compound.

Plasmids and adenoviral vectors. Adenoviruses encoding for GFP, Flag–HA–PGC-1α, Flag–R13-PGC-1α, control and *Sirt1* shRNAs were described previously[9]. Adenoviruses encoding for the different forms of AMPKα_1 subunit were a gift from P. Ferré and F. Foufelle[30]. The plasmids encoding for the mouse *Pdk4* gene promoter[20], mouse *Mcad* gene promoter[21], and the 2A-PGC-1α mutant[8] have all been described. The plasmid encoding for Flag-tagged FOXO3a was purchased from Addgene.

Cell culture, adenoviral infection and treatments. C2C12 skeletal muscle cells were grown and differentiated as described[12]. Unless otherwise stated, C2C12 were considered as myotubes after 96 h of differentiation. Differentiation medium was supplemented with 0.1 mM oleic acid. Adenoviral infections of C2C12 myocytes were performed after 48 h of differentiation. Cells were washed with PBS and left for 1 h in serum-free DMEM 4.5 g l^{-1} glucose containing the appropriate amount of viral particles (MOI = 100 per each virus used, using GFP as control to make even the final viral amount). Then, the media was replaced with fresh differentiation media for an additional 47 h before any treatment took place. MEFs were cultured in DMEM 4.5 g l^{-1} glucose supplemented with 10% fetal calf serum (FCS). Adenoviral infection of MEFs was performed when cells reached 70% of confluency, and processed as with C2C12 myocytes but using 10% FCS DMEM medium instead of differentiation medium at the end. DMSO was used as vehicle for the different treatments. Plasmids and siRNAs were transfected using Lipofectamine 2000 (Invitrogen) and following the manufacturer's instructions. *Sirt1*$^{+/+}$ and *Sirt1*$^{-/-}$ cells were a gift of F. Alt.

Total protein extraction. To obtain total protein extracts from cellular samples, cells were rapidly washed with ice-cold PBS before adding cold lysis buffer (25 mM Tris HCl pH = 7.9, 5 mM $MgCl_2$, 10% glycerol, 100 mM KCl; 1% NP40; 0.3 mM dithiothreitol, 5 mM sodium pyrophosphate, 1 mM sodium orthovanadate, 50 mM sodium fluoride, containing freshly added protease inhibitor cocktail (Calbiochem)). For acetylation studies, 5 mM nicotinamide and 1 mM sodium butyrate were added to the buffer. After 1 min, cells were scraped, transferred into an Eppendorf tube and left on ice for 5 more minutes. Then cells were homogenized with a 25-gauge needle, left for 5 more minutes on ice and centrifuged at 13,000 r.p.m. for 10 min. The supernatant was collected and kept at −80 °C.

Nuclear extracts. Nuclear extracts from gastrocnemius muscles were obtained as described previously[12].

Immunoprecipitation and western blot. Routinely, 500 μg of protein from cultured cells or 2 mg of protein from muscle samples (total lysates or nuclear extracts) were used for immunoprecipitation. Forty microlitres of protein G-sepharose re-suspended in lysis buffer were used for pre-clearing the sample and immunoprecipitation after conjugating the beads with 3–5 mg of antibody. The resulting immunoprecipitate was boiled with 50 μl of Laemmli sample buffer (LSB) and used for Western blot applications. For immunoprecipitation using rabbit polyclonal antibodies, protein-A-sepharose beads were used instead of Protein-G-conjugated beads. Western blot and protein detection was performed as described previously[12].

Gene expression analysis. RNA was extracted using TRIzol reagent (Invitrogen). Complementary DNA was generated using Superscript II enzyme (Invitrogen) and quantitative real-time PCR was performed as described previously[12] using acidic ribosomal protein (ARP) to normalize the expression. The oligonucleotides primers used for PCR analysis are provided at the end of the section.

Oxygen consumption. C2C12 myotubes or MEF cells were incubated for 5 h per day with AICAR during 2 days, in the presence of 0.1 mM oleic acid. Then oxygen consumption was measured using Seahorse Biotechnology XF24 equipment (Seahorse Bioscience Inc.) as described[31].

Oleate oxidation. The estimation of oleate oxidation rates was performed as described previously[32].

Reporter gene assays. C2C12 myocytes were transfected in 48-well plates at 90% of confluence with Lipofectamine 2000 (Invitrogen) following the manufacturer's instructions. Cells were left for 5 h with the DNA-Lipofectamine mix, and the corresponding adenoviruses were added (each adenovirus at MOI 100) for the last hour of transfection. Then, the medium was removed and replaced by differentiation medium supplemented with 0.1 mM oleic acid for 36 h before treatment with AICAR or vehicle for 12 h. For MEFs, the protocol was similar, but replacing the transfection medium by DMEM 4.5 g l^{-1} glucose 10% FCS supplemented with 0.1 mM oleic acid. Firefly luciferase activity was measured and normalized to β-gal activity (always transfected simultaneously). Empty pGL3basic reporter gene vector and pCDNA.3.1 vector were used as control vectors. pGL3-PGC-1α 2-kb promoter was purchased from Addgene. The pcDNA.3.1 HA–PGC-1α plasmid was generated in P.P.'s laboratory. pcDNA–Flag–SIRT1 plasmid was developed in our own laboratory. Reporter constructs for *Pdk4* and *Mcad* promoters were produced by D. P. Kelly's laboratory.

Measurement of SIRT1 activity. Experiments testing the direct effects of AICAR and metformin on SIRT1 activity were performed as described[28].

NAD^+/NADH measurements. NAD^+ and NADH nucleotides were directly measured as described before[33]. In brief, whole tibialis anterior muscles or two 10-cm dishes of C2C12 myotubes were homogenized in 200 μl of acid extraction buffer to measure the NAD^+ concentration, or 200 μl of alkali extraction to obtain NADH concentration. Then, homogenates were neutralized and the concentration of nucleotides was measured fluorimetrically after an enzymatic cycling reaction using 5 μl of sample. Values for both nucleotides were detected within the linear range. NAD^+/NADH ratios were calculated by comparing the ratios obtained from each animal (randomly, one tibialis was used for NAD^+ measurements and the other for NADH) or from parallel cell dishes in each experiment. The ratios obtained from different animals or individual cell culture experiment ratios were then used as individual values to calculate the mean and standard error.

Glycogen measurement. Muscle pieces (15–20 mg) were hydrolysed in 250 μl of 2 M HCl at 95 °C for 2 h. The solution was then neutralized with 250 μl 2 M NaOH, and the resulting free glycosyl units were assayed spectrophotometrically using a hexokinase-dependant assay kit (Amresco).

Protein kinase assays. For protein kinase assays on full-length SIRT1 and NAMPT, Flag-tagged proteins were produced using a coupled *in vitro* transduction and translation system (TNT, Promega Corporation). Active AMPK and SAMS peptide, as positive control substrate for AMPK, were purchased from Upstate Biotechnology. AMPK was mixed with either Flag–SIRT1, Flag–NAMPT, control vector or SAMS peptide (200 mM) in a solution containing 30 mM HEPES pH 7.4, 0.65 mM dithiothreitol, 0.02% Brij-35, 10 mM MgAc and 0.2 mM AMP. The reaction started by the addition of 0.1 mM ATP (containing [γ^{32}P]ATP at 1,000 c.p.m. pmol^{-1}), and was stopped after 20 min by adding 5 μl of 3% phosphoric acid, and 15 μl of the reaction mix were transferred to a piece of P81 phosphocellulose Whatmann paper and washed extensively with phosphoric acid solution. Then, the paper was dried with acetone and radioactivity was counted by Cherenkov counting. The rest of the reaction mix was diluted in LSB and boiled for 5 min. Western blots were performed to ensure the correct presence of the proteins in the mix (data not shown). For kinase assays on different GST–SIRT1 fragments and GST–PGC-1α 1–400 (as positive control), proteins were expressed in bacteria (BL21 strain; Invitrogen) and purified by using glutathione–Sepharose 4B beads (GE Healthcare, 17-0756-01). *In vitro* kinase assays were carried out according to the manufacturer's specifications (Millipore, 14-305). Briefly, recombinant protein was incubated with 32 mM HEPES pH 7.4, 0.01% Brij-35, 18.75 mM $MgCl_2$, 0.15 mM AMP, 0.125 mM ATP, 2.5 mCi [γ^{32}P]ATP and 0.65 mM dithiothreitol in the presence or absence of 200 ng activated AMPK for 30 min at 30 °C. The glutathione beads were then washed twice and eluted protein was analysed by SDS–PAGE and radiolabelled phosphate incorporation was assessed by autoradiography. Protein levels were determined by Coomassie blue staining.

Oligonucleotide primer list. Acidic ribosomal protein: reverse AAAGCCTGGAAGAAGGAGGTC, forward AGATTCGGGATATGCTGTTGG; *Pgc-1α*: reverse GGGTTATCTTGGTTFFCTTTATG, forward AAGTGTFFAAC TCTCTGGAACTG; *Pgc-1β*: reverse TGGAGACTGCTCTGGAAGGT, forward TGCTGCTGTCCTCAAATACG; *Nrf1*: reverse GATGACCACCTCGACCGTTT, forward CGGAGTGACCCAAACTGAAC; *Esrra*: reverse CACAGCCTCAGCAT CTTCAA, forward ACTGCCACTGCAGGATGAG; *Ppara*: reverse TTGAAGGA GCTTTGGGAAGA, forward AGGAAGCCGTTCTGTGACAT; *Pparb/d*: reverse ACTGGCTGTCAGGGTGGTTG, forward AATGCGCTGGAGCTCGATGAC; *Tfam*: reverse ATGTCTCCGGATCGTTTCAC, forward CCAAAAAGACCTCGT TCAGC; *Cyc*: reverse TCCATCAGGGTATCCTCTCC, GGAGGCAAGCATAAGA CTGG; *Cox4*: reverse GCTCGGCTTCCAGTATTGAG, forward AGAAGGAA ATGGCTGCAGAA; *Atp5g1*: reverse AFTTGGTGTGGCTGGATCA, forward GCTGCTTGAGAGATGGGTTC; mitofusin-2: reverse CAATCCCAGATGGCAG AACTT, forward ACGTCAAAGGGTACCTGTCCA; *Cpt1b*: reverse GCACCCAG ATGATTGGGATACTGT, forward TTGCCCTACAGCTGGCTCATTTCC; *Pdk4*: reverse GGAACGTACACAATGTGGATTG, forward ATCTAACATCGCCAGAA TTAAACC; *Mcad*: reverse AGCTGATTGGCAATGTCTCCAGCAAA, forward GATCGCAATGGGTGCTTTTGATAGAA; *Glut4*: reverse AGGTGAAGATGAAG AAGCCAAGC, forward CTTCTTTGAGATTGGCCCTGG; *Sod1*: reverse TTGTTTCTCATGGACCACCA, forward AGGCTGTACCAGTGCAGGAC; *Nampt*: reverse AGTGGCCACAAATTCCAGAGA, forward CCGCCACAGTA TCTGTTCCTT.

30. Woods, A. *et al.* Characterization of the role of AMP-activated protein kinase in the regulation of glucose-activated gene expression using constitutively active and dominant negative forms of the kinase. *Mol. Cell. Biol.* **20,** 6704–6711 (2000).
31. Watanabe, M. *et al.* Bile acids induce energy expenditure by promoting intracellular thyroid hormone activation. *Nature* **439,** 484–489 (2006).
32. Pich, S. *et al.* The Charcot-Marie-Tooth type 2A gene product, Mfn2, up-regulates fuel oxidation through expression of OXPHOS system. *Hum. Mol. Genet.* **14,** 1405–1415 (2005).
33. Lin, S. S., Manchester, J. K. & Gordon, J. I. Enhanced gluconeogenesis and increased energy storage as hallmarks of aging in *Saccharomyces cerevisiae*. *J. Biol. Chem.* **276,** 36000–36007 (2001).